J. Ocean Univ. China (Oceanic and Coastal Sea Research)
DOI 10.1007/s11802-017-3216-9
ISSN 1672-5182, 2017 16 (5): 793-802
http://www.ouc.edu.cn/xbywb/
E-mail:xbywb@ouc.edu.cn

Origins of Terrestrial Organic Matter in Surface Sediments of the East China Sea Shelf

ZHANG Hailong[1), 2)], XING Lei[1), 2)], and ZHAO Meixun[1), 2), *]

1) *Key Laboratory of Marine Chemistry Theory and Technology* (*Ocean University of China*), *Ministry of Education/ Qingdao Collaborative Innovation Center of Marine Science and Technology*, *Qingdao* 266100, *P. R. China*
2) *Institute of Marine Organic Geochemistry*, *Ocean University of China*, *Qingdao* 266100, *P. R. China*

(Received June 1, 2016; revised September 26, 2016; accepted November 1, 2016)

Abstract Terrestrial organic matter (TOM) is an important component of marine sedimentary OM, and revealing the origins and transport mechanisms of TOM to the East China Sea (ECS) is important for understanding regional carbon cycle. A novel approach combining molecular proxies and compound-specific carbon isotopes is used to quantitatively constrain the origins and transport mechanisms of TOM in surface sediments from the ECS shelf. The content of terrestrial biomarkers of (C_{27}+C_{29}+C_{31}) *n*-alkanes (52 to 580 ng g^{-1}) revealed a seaward decreasing trend, the $\delta^{13}C_{TOC}$ values (−20.6‰ to −22.7‰) were more negative near the coast, and the TMBR (terrestrial and marine biomarker ratio) values (0.06 to 0.40) also revealed a seaward decreasing trend. These proxies all indicated more TOM (up to 48%) deposition in the coastal areas. The Alkane Index, the ratio of C_{29}/(C_{29}+C_{31}) *n*-alkanes indicated a higher proportion of grass vegetation in the coastal area; While the $\delta^{13}C$ values of C_{29} *n*-alkane (−29.3‰ to −33.8‰) indicated that terrestrial plant in the sediments of the ECS shelf were mainly derived from C_3 plants. Cluster analysis afforded detailed estimates of different-sourced TOM contributions and transport mechanisms. TOM in the Zhejiang-Fujian coastal area was mostly delivered by the Changjiang River, and characterized by higher %TOM (up to 48%), higher %C_3 plant OM (68%−85%) and higher grass plant OM (56%−61%); TOM in the mid-shelf area was mostly transported by aerosols, and characterized by low %TOM (less than 17%), slightly lower C_3 plant OM (56%−72%) and lower grass plant OM (49%−55%).

Key words terrestrial organic matter; $\delta^{13}C$; *n*-alkanes; the East China Sea

1 Introduction

Continental shelf seas are important carbon sink because about 80% marine sedimentary organic matter is buried in the shelf and slope areas (Hedges and Keil, 1995; McKee *et al*., 2004). In addition to marine organic matter (MOM) produced in the photic zone, significant amounts of terrestrial organic matter (TOM) are transported to shelf seas by both river runoff and dust deposition. Since different-sourced OM plays different roles as carbon sink on different timescales, it is important to distinguish the origin and transport pathway of sedimentary OM in marginal seas.

The East China Sea (ECS) is one of the largest river-dominated shelf seas and TOM could be supplied by both the Changjiang River and dusts. The Changjiang River discharges 480 Mt yr^{-1} of sediments and 2−5 Mt yr^{-1} of OM to the ECS (Wu *et al*., 2004). Aerosol deposition is also a source of TOM to the ECS (Zhang *et al*., 2007), as cold-dry winter monsoon originated from Siberia can influence most of the continent and China marginal seas (An *et al*., 2000). Both rivers and dusts also transport significant amounts of nutrients to the ECS to enhance marine productivity and the burial of MOM, thus affecting the organic carbon cycle in the ECS. The deposition of nutrients from the East Asian continent into the ECS (Uematsu *et al*., 2003) is very significant, for example, dissolved inorganic nitrogen (DIN) derived from aerosol was almost equal to DIN contribution from rivers in the ECS nutrient budget (Zhang *et al*., 2007).

The origins of OM and amounts of TOM in marine sediments can be estimated using both bulk organic parameters and biomarkers (Weijers *et al*., 2009; Xing *et al*., 2014; Zhu *et al*., 2013). One study using multi-proxies indicated that TOM from the Changjiang River was transported southward along the Zhejiang-Fujian coast (Zhu *et al*., 2008). The contents of *n*-alkanes and fatty acids and $\delta^{13}C$ values of fatty acids (Wang *et al*., 2008) showed that TOM was mainly deposited in the Changjiang River Estuary (CRE) and the inner ECS shelf, controlled by the Changjiang River runoff and the Zhejiang-Fujian coastal current. These conclusions were further supported by quantitative estimates using total organic carbon (TOC) $\delta^{13}C$ and a biomarker ratio proxy of

* Corresponding author. Tel: 0086-532-66782103
E-mail: maxzhao@ouc.edu.cn

TMBR (Terrestrial and Marine Biomarker Ratio), which also indicated that TOM was mainly deposited in the CRE and Zhejiang-Fujian coastal area, but not in the mid-outer shelf of the ECS (Xing *et al*., 2011). A new study also indicated soil-derived TOM was mostly deposited in the inner estuary of the Changjiang, while vegetation derived TOM can be carried to the coastal regions (Yao *et al*., 2015). Concerning vegetation types of OM sources, lignin data from the ECS surface sediments indicated a higher proportion of herb than woody plant OM in the inner shelf of the ECS, especially at the lower latitude areas (below 31.5°N) (Yang *et al*., 2008). The $\delta^{13}C$ values of long-chain *n*-alkanes in surface sediments from 4 sites indicated that TOM was dominated by C_3 plant OM in all sites, but a higher proportion of C_3 plant OM was observed in the coastal sites than in the outer shelf sites (Guo *et al*., 2006b). A few studies also attempted to estimate the amount and fate of atmospheric-transported OM in the ECS, with one study suggesting that atmospheric deposition contributed only 0.56% of TOC to the sedimentary OM in the ECS (Deng *et al*., 2006), underscoring the need for further studies. The content and δD values of aerosol fatty acids from the Cheju Island of the ECS indicated TOM was carried by the Asia winter wind to ECS, and alkanes were dominated by C_{29} or C_{31} *n*-alkanes in most aerosol samples (Yamamoto *et al*., 2013). However, no reports have focused on both the sources and transport mechanisms of TOM in the ECS. More importantly, the lack of compound-specific $\delta^{13}C$ values of alkanes limited the estimate of C_4 plant contribution to TOM, which could overestimate marine OM contribution in sediment. The aim of this preliminary study is to employ several alkane-based proxies (especially $\delta^{13}C$) to better constrain the distribution and origins of TOM in the ECS shelf and to evaluate the mechanism of TOM transport to the ECS shelf. *n*-Alkanes are best suited for estimating both river and dust inputs as they can be carried by both pathways (Xing *et al*., 2014).

2 Materials and Methods

Five surface sediment samples (0–1 cm) from the ECS shelf (the same samples as in Xing *et al*., 2011) were collected using a box corer in April of 2006 using R/V Beidou of Yellow Sea Fisheries Research Institute, and data of TMBR, %TOC and $\delta^{13}C_{TOC}$ for these samples have been reported in Xing *et al*., 2011; twelve samples were collected in 2011 (new) using R/V Kexue 3 of Institute of Oceanology, Chinese Academy of Science (Fig.1b). All samples were stored at −20℃.

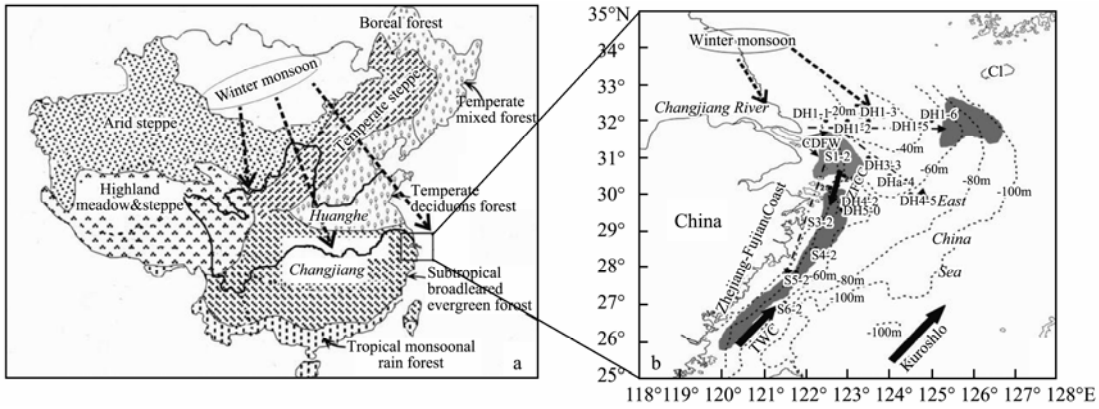

Fig.1 The direction of the East Asia Winter Monsoon wind (Fig.1a), and the surface sediment locations in the East China Sea (Fig.1b). Arrows indicate the wind directions in winter (Modified from Qiao *et al*., 2011; Yamamoto *et al*., 2013; Yi *et al*., 2006). Fig.1a shows the distributions of the vegetation types from China (Wu, 1980). Fig.1b shows a map of the sampling sites in the ECS (modified from Xing *et al*., 2011). Mud areas are marked in gray. Bathymetry contours are indicated by dashed lines (CDW: Changjiang Diluted Water; ZFCC: Zhejiang-Fujian Coastal Current; TWWC: Taiwan Warm Current; and CI: the Cheju Island).

For biomarker analysis, freeze dried sediment samples were extracted four times with organic solvent (dichloromethane/Methanol=3:1, V/V) by sonication (15 min each time), after adding an internal standard mixture containing C_{19} *n*-alkanol and *n*-$C_{24}D_{50}$. The extracts were hydrolyzed with 6% KOH in MeOH overnight and then extracted using hexane. The extracts were separated into fractions with silica gel chromatography. The non-polar lipid (containing *n*-alkanes) was eluted with 8 mL hexane, dried under a gentle N_2 stream for instrumental analyses; and the neutral lipid fraction (containing alkenones (A), dinosterol (D), and brassicasterol (B)) was eluted with 12 ml dichloromethane/methanol (95:5, v/v), dried under a gentle N_2 stream and the derivative with N, O-bis (trimethylsily)-trifluoroacetamide (BSTFA) at 70℃ for 1 h before instrumental analyses. Biomarker quantification was performed on an Agilent 6890N GC with a FID detector, using a HP-1 capillary column (50 m × 0.32 mm i.d.× 0.17 μm film thickness, J&W Scientific) and H_2 as the carrier gas at 1.2 mL min^{-1}. Oven temperature programming was 80–200℃ at 25℃ min^{-1}, 200–250℃ at 4℃min^{-1}, 250–300℃ at 1.8℃ min^{-1}, and holding at 300℃ for 15 min. The total contents of (C_{27}+C_{29}+C_{31}) *n*-alkanes are a TOM indicator and the total contents of the three marine biomarkers (A, B and D) are an indicator of marine organic matters (MOM). The TMBR, defined as (C_{27}+C_{29}+C_{31})

n-alkanes/((C_{27}+C_{29}+C_{31}) *n*-alkanes + A + B + D), was used to estimate the relative TOM contribution (Xing *et al*., 2011).

For TOC analysis, the sediment samples were freeze dried, homogenized and powdered, decalcified by reaction with 4 mol L^{-1} HCl at room temperature for about 24 h. After rinsed using demonized water several times and dried at 55℃, the carbonate-free sediment samples were measured for TOC in duplicates using Thermo Fisher Flash 2000 Elemental Analyzer (EA), with a standard deviation of ±0.02 wt% (n=6). The standard used in the EA analysis is Soil Reference (C=3.50%, Säntis Analytical AG).

$\delta^{13}C_{TOC}$ was determined on the carbonate-free samples using a Thermo Fisher Delta V mass spectrometer (continuous flow mode), with an analytical precision of less than 0.2‰ (n=6). The organic carbon isotopic ratios were reported in parts per million (‰) calculated as follows:

$$\delta^{13}C_{TOC}\ (‰) = (R_{Sample} / R_{Standard} - 1) \times 1000 . \quad (1)$$

The $\delta^{13}C$ values of C_{29} *n*-alkane were measured by gas chromatography-isotope ratio mass spectrometry (GC-IRMS). A Thermo Trace GC ULTRO was connected to a Thermo Delta V mass spectrometry *via* a GC-C III interface, using a DB-1 MS capillary column (60 m × 0.25 mm i.d. × 0.25 μm film thickness, J&W Scientific) and He as the carrier gas at 1.0 mL min^{-1}. Oven temperature programming was 60–200℃ at 15℃ min^{-1}, 200–250℃ at 4℃ min^{-1}, 250–300℃ at 1.8℃ min^{-1}, 300–310℃ at 5℃ min^{-1}, and holding at 310℃ for 5 min. *n*-Alkanes were oxidized at 980℃ and converted to CO_2. Four pulses of standard CO_2 gas, pre-calibrated against a commercial reference CO_2, were injected via the GC-C III interface to the IRMS for the calculation of $\delta^{13}C$ values of C_{29} *n*-alkane (Fig.2). A set of 15 *n*-alkanes with known $\delta^{13}C$ values from Indiana University were measured daily to ensure the accuracy of the machine. The standard deviation for duplicate analysis of the standard was < 0.4‰. The $\delta^{13}C$ values are reported with reference to the PDB standard.

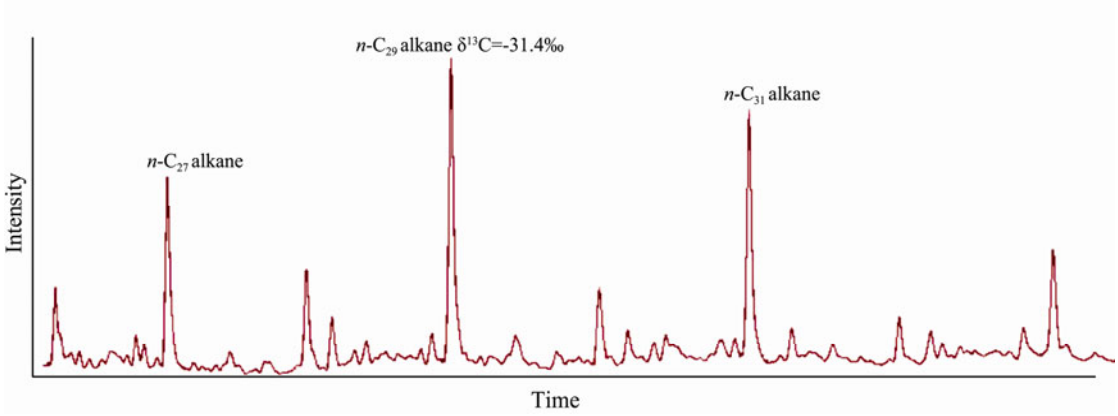

Fig.2 A representative chromatogram of alkane distribution of GC/C-IRMS, showing the $\delta^{13}C$ value of *n*-C29 alkane.

Cluster analysis was performed using the SPSS 16.0 program for Windows (SPSS Inc., Chicago, Illinois).

3 Results

3.1 TOM Proxies

Plotted in Fig.3 are the spatial distribution of TOC, ∑*n*-alkanes (C_{27}+C_{29}+C_{31}) content, TOC normalized ∑*n*-alkanes, $\delta^{13}C_{TOC}$, %TOM estimated from $\delta^{13}C_{TOC}$, and TMBR.

TOC varied from 0.16 to 0.55% with a seaward decreasing trend (Fig.3a). The content of ∑*n*-alkanes ranged from 52 to 580 ng g^{-1} (Fig.3b), also with a seaward decreasing trend. The spatial distribution of TOC-normalized ∑*n*-alkanes content (Fig.3c) is similar to those of TOC and ∑*n*-alkanes content. $\delta^{13}C_{TOC}$ values varied from −20.6‰ to −22.7‰ (Fig.3d; Table 1), similar to previous results (−20.1‰ to −22.4‰) in the ECS sediments (Kao *et al*., 2003). The marine end-member $\delta^{13}C$ value is usually −20‰ (Hedges *et al*., 1997; Weijers *et al*., 2009), and the lowest $\delta^{13}C$ values in our sample is also around −20‰, very close to the global average value. Thus, we selected −20‰ as the end-member $\delta^{13}C$ values for MOM. For terrestrial end-member $\delta^{13}C$ values, previous results showed that OM (mostly terrestrial) $\delta^{13}C$ values in the main stream of the Changjiang River ranged from −26.6‰ to −24.4‰ (an average of −25.6‰), similar to that of surface soils along the Changjiang riverbank (−28.9‰ to −24.3‰) (Wu *et al*., 2007). Based on these results and global studies, −25.6‰ is used as the end-member $\delta^{13}C$ values for TOM. %TOM estimated based on $\delta^{13}C_{TOC}$ showed higher values near and south of the CRE, and a seaward decreasing trend (Fig.3f), with a range of 12%–48%. TMBR values ranged from 0.06 to 0.40 (Table 2; Fig.3d) with higher values near and south of the CRE, and a seaward decreasing trend, similar to previous results in both values (0.06 to 0.48) and spatial trend for the ECS (Xing *et al*., 2011; Yang *et al*., 2015).

3.2 Vegetation Proxies

The $\delta^{13}C$ values of C_{29} *n*-alkane ranged from −29.3‰ to −33.8‰ with a seaward increasing trend (Fig.4a). The percentage of C_3 (%C_3) plant OM contribution is calculated by choosing $\delta^{13}C$ end-member values of −36‰ and −21‰ for C_3 plant and C_4 plant, respectively (Zhang *et al*., 2003b; Zhao *et al*., 2000). The %C_3 plant OM contribu-

tion ranged from 56% to 85% (Fig.4b; Table 2), with higher values near and south of the Changjiang Estuary, and a seaward decreasing trend.

The Alcohol Index (C_{26} *n*-alkanol/ C_{29} *n*-alkane) values varied from 1.13 to 2.95 (Table 2) with a seaward increasing trend (Fig.4c). The Alkane Index (A.I.), the ratio of $C_{29}/(C_{29}+C_{31})$ *n*-alkanes, varied from 0.39 to 0.51 (Table 2) in our samples with an increasing trend from the coast to offshore (Fig.4d).

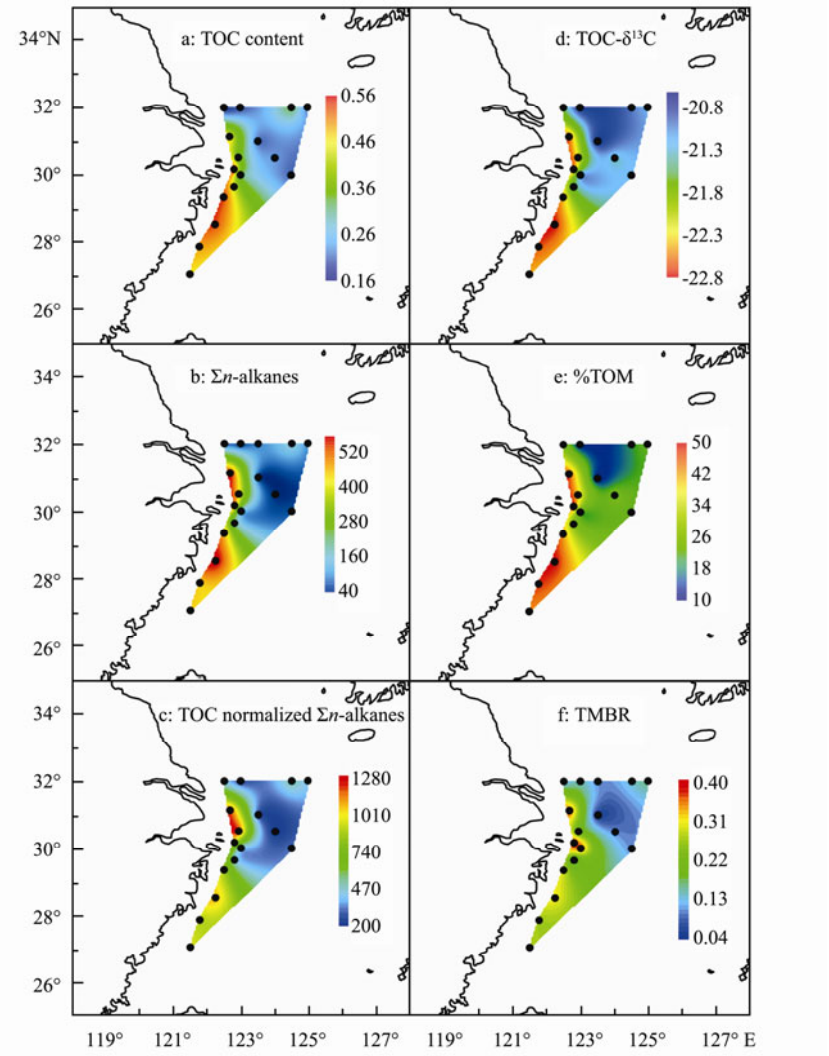

Fig.3 The spatial distribution of TOC (a, %), ∑*n*-alkanes (C_{27}+C_{29}+C_{31}) content (b, ng g^{-1}), TOC normalized ∑*n*-alkanes (c, ng/g/%TOC), $\delta^{13}C_{TOC}$ (d, ‰), %TOM (e) estimated from $\delta^{13}C_{TOC}$, and TMBR (f).

Table 1 Values of $\delta^{13}C_{TOC}$, $\delta^{13}C$ of C_{29} *n*-alkane, TOC content (%TOC), ∑*n*-alkanes (ng g^{-1}) (C_{27} +C_{29}+C_{31} *n*-alkanes), ∑A+B+D (ng g^{-1}) (Alkenones + Brassisterol + Dinosterol). nd is not detected. The data of ∑*n*-alkanes, ∑A+B+D and $\delta^{13}C_{TOC}$ in five sites (the S sites in Fig.1b, Table 1) have been reported previously (Xing *et al.*, 2011)

Sites	$\delta^{13}C_{TOC}$	$\delta^{13}C$ C_{29} *n*-alkane	%TOC	∑*n*-alkanes	∑A+B+D
DH1-1	-21.5	-31.4	0.16	66	499
DH1-2	-20.7	-30.3	0.20	53	292
DH1-3	nd	-31.8	nd	97	810
DH1-5	-21.0	-30.6	0.33	173	1044
DH1-6	-21.2	-30.6	0.22	93	457
DH3-3	-20.6	-30.6	0.22	57	953
DHa-4	-21.3	-29.3	0.24	52	443
DH4-5	-21.2	-30.9	0.21	71	604
S1-2	-22.6	-32.5	0.47	570	926
21	-22.2	-31.2	0.35	439	1778
25	-22.7	-31.2	0.55	523	782
DH4-2	-21.1	-31.7	0.31	120	199
DH5-0	-21.5	-31.8	0.44	197	857
S3-2	-22.4	-33.8	0.53	475	1105
S4-2	-22.7	-33.0	0.53	580	1265
S5-2	-22.6	-32.7	0.49	447	1223
S6-2	-22.4	-33.2	0.46	452	1168

Table 2 Values of TMBR, the percentage of C_3-plant (%C_3), the ratio of C_{26} *n*-alkanol/C_{29} *n*-alkane, the percentage of woody plant (C_{29}/(C_{29}+C_{31}) *n*-alkane). nd is not detected. The data of TMBR in five sites (the S sites in Fig.1b, Table 1) have been reported previously (Xing *et al*., 2011)

Sites	TMBR	%C_3	C_{26} *n*-alkanol/C_{29} *n*-alkane	%woody
DH1-1	0.12	69	1.79	0.46
DH1-2	0.15	62	1.82	0.45
DH1-3	0.11	72	1.78	0.49
DH1-5	0.14	64	1.50	0.45
DH1-6	0.17	64	1.50	0.47
DH3-3	0.06	64	1.82	0.50
DHa-4	0.11	56	2.18	0.48
DH4-5	0.11	66	1.13	0.51
S1-2	0.38	77	2.52	0.43
21	0.20	68	1.78	0.44
25	0.40	68	1.77	0.42
DH4-2	0.38	71	1.88	0.42
DH5-0	0.15	72	1.27	0.39
S3-2	0.30	85	2.36	0.44
S4-2	0.31	80	2.64	0.41
S5-2	0.27	78	2.95	0.42
S6-2	0.28	82	2.24	0.41

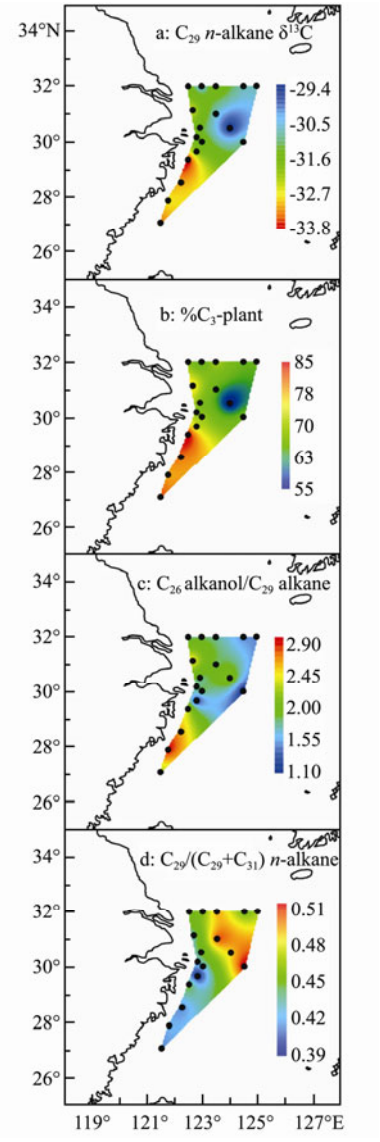

Fig.4 Spatial distribution of $\delta^{13}C$ of C_{29} *n*-alkane (a, ‰), the percentage of C_3 plant OM (b, %), the ratio of C_{26} *n*-alkanol/C_{29} *n*-alkane (c), and the ratio of C_{29}/(C_{29}+C_{31}) *n*-alkanes (d).

4 Discussion

Sediment OM burial plays different roles as carbon sinks due to variations of composition, age and origins (Feng *et al*., 2013; Hedges and Keil, 1995; Pearson *et al*., 2001; Xing *et al*., 2014), thus it is necessary to distinguish the origins and transport pathways of sedimentary OM in marginal seas. We use alkane-based proxies to evaluate mechanisms controlling the spatial distributions of TOM, C_3 versus C_4 plant OM and woody versus grass OM, in the ECS.

4.1 Spatial Distribution of Terrestrial Organic Matter

4.1.1 Spatial distribution of %TOM

The $\delta^{13}C$ of TOC has been traditionally used to determine the relative amounts of TOM in marine sediments. The %TOM calculated from $\delta^{13}C_{TOC}$ value in our samples showed a seaward decreasing trend (Fig.3e), with high values (19%–48%) in the coastal area, and lower values (12%–26%) in the mid-shelf area; and this spatial trend as well as the %TOM ranges are consistent with previous estimates using $\delta^{13}C_{TOC}$, which showed %TOM values ranging from 48% along the coast (Xing *et al*., 2011; Yao *et al*., 2015) to near 0% in the mid-outer shelf (Xing *et al*., 2011). Using the new TMBR index, the %TOM in our samples ranged from 6% to 40%, with the highest values near the CRE and the lowest value in mid-shelf area (Fig. 3f), and both the values and the spatial patterns are also broadly similar to those reported for this region (Xing *et al*., 2011; Wu *et al*., 2013).

For this study, the %TOM values estimates from $\delta^{13}C_{TOC}$ and TMBR are similar, and also in agreement with previously reported values for this region (Xing *et al*., 2011). The highest %TOM values are 40%–48%, occurring near the CRE. The values and location of higher %TOM were both in agreement with results from multi- proxy estimates for the ECS (Yao *et al*., 2015). In

the Yellow Sea, previous estimates of %TOM from $\delta^{13}C_{TOC}$ ranged from 0 to 43%, with the highest values near the Old Huanghe River delta (Xing *et al*., 2014); however, %TOM estimated from TMBR had higher values with a range of 12%–85%, with the highest values also near the Old Huanghe River delta (Xing *et al*., 2014). The consistence of the present result with previous work provided additional evidence that these proxies are robust, and can be the beginning for more spatially and temporally high resolution studies of OM sources in marginal seas.

4.1.2 Spatial distribution of C_3 and C_4 plant organic matter

C_3 and C_4 plants are the major terrestrial vegetation types, thus estimating C_3 and C_4 OM distribution in marine sediments is important to evaluate the source regions and transport mechanisms of different TOM in sediments and their roles in the carbon cycle. On land, $\delta^{13}C_{TOC}$ has been used to estimate C_3 and C_4 plant distribution, however, the contribution of MOM with heavier $\delta^{13}C$ values (Hedges and Oades, 1997) would limit the use of $\delta^{13}C_{TOC}$ index to distinguish C_3 and C_4 plant OM in marine sediments.

The $\delta^{13}C$ measurements of biomarkers such as *n*-alkanes provide more specific information on C_3 and C_4 OM contribution. The $\delta^{13}C$ value of C_3 plant alkanes has a range of −32‰ to −39‰ and that of C_4-plant alkanes has a range of −18‰ to −25‰ (Collister *et al*., 1994). By choosing $\delta^{13}C$ end-member values of −36‰ and −21‰ for C_3 plant and C_4 plant, respectively (Zhang *et al*., 2003b; Zhao *et al*., 2000), the percentage of C_3 plant OM contribution ($\%C_3$) is calculated by the following equation:

$$\%C_3\text{-plant}\times(-36‰)+(1-\%C_3\text{-plant})\times(-21‰)=\delta^{13}C_{measured}. \quad (2)$$

The $\%C_3$ plant OM ranged from 56% to 85% (Table 2). These calculations indicate that higher C_3 plant OM contribution occurred in the inner shelf varying from 68%–85%, while C_4 plant OM contribution increased seaward (Fig.4b). Our results are broadly in agreement with limited *n*-alkane $\delta^{13}C$ data for 4 sites which indicated that $\%C_3$ plant contribution was higher in coastal zone (83%–90%) than that in outer shelf (70%–75%) of the ECS (Guo *et al*., 2006b). However, our expanded data set from 17 sites in comparison of the 4 sites affords better constraints on both the value ranges (56%–85%) and spatial pattern of C_3 plant OM contribution, which can be used to evaluate both sources and transport mechanisms of TOM to the ECS. For comparison, %TOM and C_3% had broadly similar spatial patterns with higher values in the coastal regions, but %TOM had two high value areas in the Changjiang River Estuary and Zhejiang coastal area (Fig.3e), while C_3% only had one high value area in the Zhejiang coastal area. The difference is related to the different meaning of the proxies. %TOM is calculated using TOC $\delta^{13}C$, which includes both C_3 and C_4 plant OM; while C_3% is calculated from compound-specific $\delta^{13}C$, and it is used to specifically estimate C_3 plant OM contribution to TOM. Thus, this comparison suggested that Zhejiang coastal area had more C_3 OM sources, such as from local small rivers.

The ratio of C_3/C_4 plant OM in marine sediments reflected terrestrial vegetation types as well as the relative amount of TOM transported by different pathways (Zhao *et al*., 2000). Previous study indicated the $\%C_4$ plant in the Chinese Loess Plateau was about 27% (Liu *et al*., 2002). The $\delta^{13}C$ values of soil OM along an S-N transect from the Qinling Mountain to Hanhayn Huryee (34°N to 52°N) indicated that C_3 plants were the major vegetation type (Feng *et al*., 2008). The $\delta^{13}C$ of surface soil OM in northwestern China (Zhang *et al*., 2003a; Lu *et al*., 2004) and the $\delta^{13}C$ values of plant OM from southern China (Ehleringer *et al*., 1987) also indicated that C_3 plants were the major vegetation type. The $\delta^{13}C$ in grazer wool revealed that only 19% of C_4 plants existed in the Inner Mongolia steppe vegetation (Auerswald *et al*., 2009). Similarly, the $\delta^{13}C$ values of TOC and long chain *n*-alkanes from surface soils showed that C_3 plants were dominant in high-latitude (40°N–52°N) and low-latitude (18°N–31°N) areas (Rao *et al*., 2008; Wang *et al*., 2000). However in the mid-latitude area (31°N–40°N), the relative contribution of C_4 plant was higher despite the overall domination of C_3 plants (Rao *et al*., 2008; Wang *et al*., 2000). $\delta^{13}C$ values of particulate organic carbon (POC) from the Changjiang River ranged from −25.1‰ to −26.8‰, similar to $\delta^{13}C$ values of land plants in the Changjiang drainage area (−24.1‰ to −28.8‰) (Wu *et al*., 2007), indicating that the majority of terrestrial plants derived from the Changjiang River were C_3 plants. Thus, C_3 plants are the dominating vegetation for northern China and this isotope signal was carried to the marginal seas by river discharges.

Dust depositions into the ECS sediments are mainly derived from the mid-latitude regions of western China (30°N–40°N) and are transported by the East Asian Winter Monsoon (EAWM) winds (Uematsu *et al*., 2003). Thus, EAWM-carried TOM would contain a higher proportion of C_4 vegetation from mid-latitude region (30°N–40°N) (Wang *et al*., 2000; Rao *et al*., 2008). $\delta^{13}C$ values of C_{31} and C_{29} *n*-alkanes from atmospheric aerosols collected in Qingdao revealed that the relative contribution of C_4 plant OM ranged from 17% to 20% (Guo *et al*., 2006a).

In addition to the origins, the degradation of *n*-alkanes could also influence their $\delta^{13}C$ values. Lighter carbon isotope (^{12}C) is more prone to degradation reactions, resulting in more positive ^{13}C values of the remaining fraction in sediments (Games *et al*., 1978; Gelwicks *et al*., 1994). In our samples, the alcohol index (C_{26} *n*-alkanol/C_{29} *n*-alkane ratio) was used to estimate the degradation extent of OM. This index was proposed based on the assumption that C_{26} *n*-alkanol and C_{29} *n*-alkane are both originated from higher land plants (Eglinton and Hamil-

ton, 1967), but C_{26} *n*-alkanol is more labile than C_{29} *n*-alkane; and thus the alcohol index is affected by degradation in different environment. Consequently, lower alcohol index values could indicate more oxic conditions and more OM degradation (Cacho *et al*., 2000). The spatial distribution of the alcohol index in our samples had a decreasing trend away from the coast (Fig.4c), suggesting increased degradation of OM offshore. Since increased degradation could result in more positive $\delta^{13}C$ values of C_{29} *n*-alkane, this could result in an overestimate of C_4 plant OM contribution in the mid-shelf areas. Another reason for higher C_4% in offshore sediments could be that sediment values were time-averaged over decades, which could imply that the C_4% in TOM in the past was higher. Finally, most aerosol samples contained some anthropogenic alkane contributions with lower $\delta^{13}C$ values which would result in lower estimates of C_4 OM contributions. Our preliminary results can only be further evaluated by future comprehensive studies of both aerosol and marine sediments.

4.1.3 Spatial distribution of woody and grass plant organic matter

The relative amounts of the individual *n*-alkanes differ among different vegetation types, with woody plants more dominated by the C_{27} or C_{29} *n*-alkanes and grass often dominated by C_{31} *n*-alkane (Eglinton and Hamilton, 1967). Both the average chain length (ACL) and the Alkane Index (A.I.) have been used for estimating vegetation types, but the A.I. provides a ratio and thus a more quantitative measure. Hence, the A.I., defined as $C_{29}/(C_{29}+C_{31})$ *n*-alkane in our study, has also been used to estimate the changes in terrestrial vegetation type (Cranwell, 1973; Zhang *et al*., 2003b; Zhao *et al*., 2000). Our results reveal a higher proportion of grass plant OM was deposited near the CRE while a higher proportion of woody plant OM was deposited in the mid-shelf region (Fig.4D), broadly in agreement with lignin data from the ECS surface sediments which indicated a higher proportion of herb than woody plant OM in the inner shelf of the ECS, especially at the lower latitude areas (below 31.5°N) (Yang *et al*., 2008).

This spatial pattern likely reflected land vegetation types and transportation pathways of plant OM. Although forest is the major land vegetation type in the middle and lower reaches of the Changjiang River (Wu, 1980; Liu, 1988), lignin evidence indicated that grass plant OM carried by the Changjiang River was the major contributors to terrestrial plant OM in surface sediments of the ECS shelf (Yang *et al*., 2008). $\delta^{13}C$ values of POM from the Changjiang River were similar to those of TOC in soils around the Changjiang River where more grass plants grew (Wu *et al*., 2007). Hence, TOM from the Changjiang River is expected to have low A.I. values (more grass plant OM). Besides river input, aerosols are the other source of TOM input into the ECS. C_{29} *n*-alkane was the dominant alkane homologue in aerosols from northern China (Beijing and Qingdao) (Feng *et al*., 2006; Guo *et al*., 2003), and C_{29} and C_{31} *n*-alkanes were the most abundant in aerosols from central China (Shanghai), while C_{31} *n*-alkane was dominant in aerosols from southern China (Guangzhou) (Feng *et al*., 2006). These results suggest that long-chain *n*-alkane transported by aerosols from mid-latitude land region into the mid-shelf areas of the ECS likely contain more C_{29} *n*-alkane. As a result, increased $C_{29}/(C_{29}+C_{31})$ *n*-alkane values in mid-shelf samples are likely linked with weaker influence of the Changjiang Diluted water and relatively high TOM contribution derived from aerosols, which carry more woody plant OM.

4.2 Quantitative Estimates of TOM Origins and Transport Mechanisms

To further evaluate the roles of the Changjiang River and aerosols on the transport and spatial distribution of TOM with different origins, cluster analysis was performed using the datasets containing TMBR, $C_{29}/(C_{29}+C_{31})$ *n*-alkane and $\%C_3$-plant OM. As shown in Fig.5, the sites were easily separated into two areas (Figs.5a and 5b).

More quantitative estimates of woody versus grass OM contributions can be achieved by assigning end-member values. All woody plants are C_3 plants, while grass plants contain both C_3 plants and C_4 plants. We use the ratio of $C_{29}/(C_{29}+C_{31})$ *n*-alkane to represent the contribution of woody vegetation (Table 2), and calculate the relative contributions of C_3 grass and C_4 grass vegetation using the following formula.

$$C_3\text{-grass} = C_3\text{-plant}\% - \text{woody}\%, \quad (3)$$

$$C_4\text{-grass} = 1 - C_3\text{-plant}\%. \quad (4)$$

The percentage ranges of woody, C_3-grass and C_4-grass OM are 39%–51%, 8%–41%, and 15%–44%, respectively (Fig.5c). At the mid-shelf sites, C_4-grass OM contribution is high with a range of 28%–44% (blue circle, Figs.5b and 5c), while relatively low C_4-grass OM contribution is found with a range of 15%–32% at near-shore sites (red circle, Fig.5b and 5c). Seaward increasing contribution of woody OM is also found with a range of 45% –51% in the mid-shelf area (blue circle, Figs.5b and 5c) and a range of 39%–44% near-shore (red circle, Figs.5b and 5c). In contrast, the contribution of C_3-grass OM is higher in the coastal area (24%–41%) than that in the mid-shelf area (8%–23%) (Figs.5b and 5c). Our results are consistent with previous results (Yang *et al*., 2008).

To summarize, the Zhejiang-Fujian coastal zone (red circle) was characterized by higher TMBR values (0.20–0.40) (Fig.3f) and higher %TOM (Fig.3e), higher $\%C_3$ plant OM contribution (68%–85%) (Fig.4b) and higher grass plant OM contribution (56%–61%) (Fig.4d). In contrast, the mid-shelf area (blue circle) was characterized by low TMBR values (0.06–0.17), slightly lower C_3 plant OM contribution (56%–72%) and lower grass plant OM contribution (49%–55%).

These spatial variations reflected the vegetation types of the sources areas and the main transportation pathways of TOM. In the coastal area which includes the CRE and

the Zhejiang-Fujian Coasts (red circle area, Fig.5b), TOM input was mainly carried by the Changjiang River. Thus in this region, the %TOM was higher, dominated by C_3 plant OM and a higher proportion of grass vegetation OM. In the mid-shelf area (blue circle area, Fig.5b), aerosol carried TOM deposition was important. TOC was dominated by marine OM, so %TOM was lower but containing a higher proportion of woody OM and a higher proportion of C_4 grass OM. Another important factor for the spatial patterns is the regional current system forced by seasonal reversed monsoons. During the winter, strong coastal currents would transport Changjiang River delivered terrestrial OM southward to the Zhejiang-Fujian Coasts. On the other hand during the summer, the Changjiang Diluted Water would carry more terrestrial OM to the mid-shelf area. Future studies of modern samples combining both chemical and physical parameters are needed for quantitative estimates of the role of current system on terrestrial OM spatial distribution.

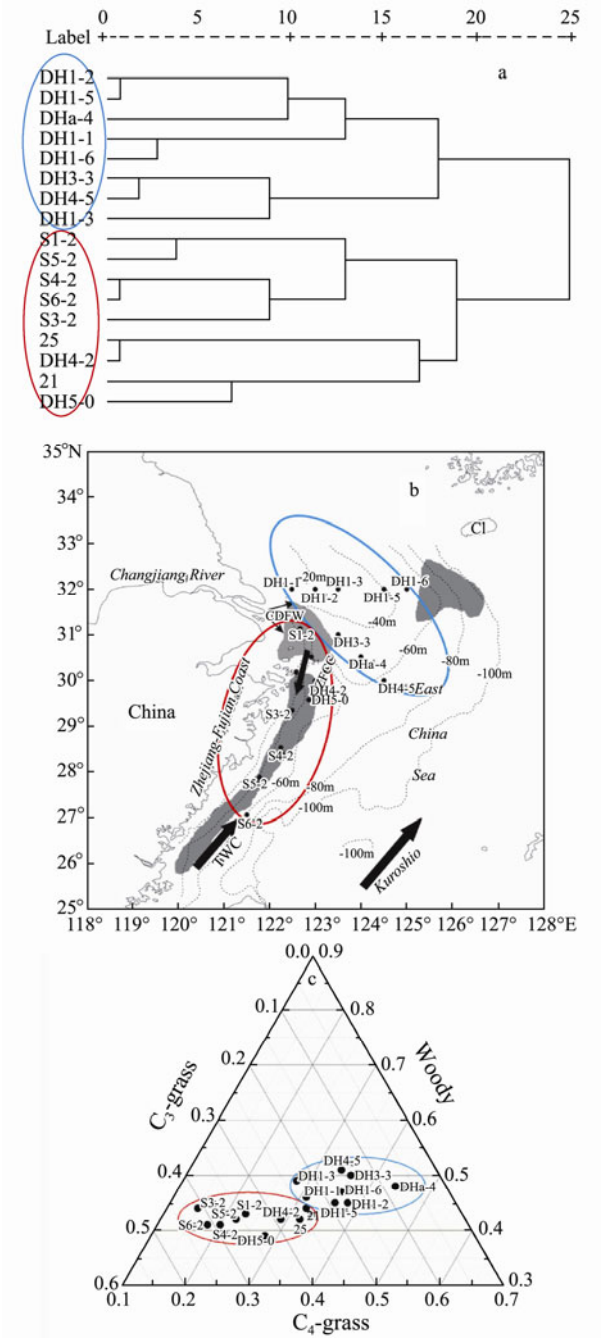

Fig.5 Cluster analysis of TOM and the spatial distribution of different-sourced OM. The blue circle defines the sites in the offshore area, and the red circle defines the sites in the inner shelf of ECS. Relative contribution of woody, C_3-grass and C_4-grass. Blue circle indicates the sites in the off-shore area, and red circle indicates the sites in the inner shelf of ECS.

5 Conclusions

1) A multi-proxy approach has been used to more quantitatively estimate OM origins in surface sediments of the ECS shelf. %TOM ranged from 6% to 48%. Among TOM, woody plant OM accounted for 39%–51%, C_3 grass OM for 8%–41%, and C_4 grass OM for 15%–44%.

2) A clear spatial contrast is observed in the different-sourced OM distributions. The Zhejiang-Fujian coastal area was characterized by higher %TOM, higher %C_3 plant OM and higher grass plant OM contribution, while the mid-shelf area was characterized by low %TOM, slightly lower C_3 plant OM and lower grass plant OM contribution.

3) Both the sources and transportation pathways are important in controlling different-sourced OM distributions in shelf sediment. In the coastal areas, the Changjiang River was the main carrier of OM from the river basin, resulting in higher %TOM, dominated by C_3 plant OM and a higher proportion of grass vegetation OM. Aerosols-carried OM from the mid-latitude land region was important in TOM depositions the mid-shelf area, resulting in a higher proportion of woody OM and a higher proportion of C_4 grass OM. Dust transported TOM could be up to 17% of sediment TOC for the mid-shelf region.

Acknowledgements

This study was support by the Key Laboratory of Marine Hydrocarbon Resources and Environmental Geology, Ministry of Land and Resources (No. MRE201301), the National Natural Science Foundation of China (No. 41506087) and the '111' Project (No. B13030). This is MCTL contribution #116.

References

An, Z., Porter, S., Kutzbach, J., Wu, X., Wang, S., Liu, X., Li, X., and Zhou, W., 2000. Asynchronous holocene optimum of East Asian monsoon. *Quaternary Science Reviews*, **19** (8): 743-762, DOI: 10.1016/S0277-3791(99)00031-1.

Auerswald, K., Wittmer, M., Mannel, T., Bai, Y. F., Schaufele, R., and Schnyder, H., 2009. Large regional-scale variation in C_3/C_4 distribution pattern of Inner Mongolia steppe is revealed by grazer wool carbon isotope composition. *Biogeosciences*, **6** (5): 795-805, DOI: 10.5194/bg-6-795-2009.

Cacho, I., Grimalt, J. O., Sierro, F. J., Shackleton, N., and Canals, M., 2000. Evidence for enhanced Mediterranean ther-

mohaline circulation during rapid climatic coolings. *Earth and Planetary Science Letters*, **183** (3-4): 417-429, DOI: 10.1016/S0012-821X(00)00296-X.

Collister, J. W., Rieley, G., Stern, B., Eglinton, G., and Fry, B., 1994. Compound-specific $\delta^{13}C$ analysis of leaf lipids from plants with differing carbon dioxide metabolism. *Organic Geochemistry*, **21** (6-7): 619-627, DOI: 10.1016/0146-6380(94)90008-6.

Cranwell, P. A., 1973. Chain-length distribution of *n*-alkanes from lake sediments in relation to post-glacial environment change. *Freshwater Biology*, **3** (3): 259-265, DOI: 10.1111/j.1365-2427.1973.tb00921.x.

Deng, B., Zhang, J., and Wu, Y., 2006. Recent sediment accumulation and carbon burial in the East China Sea. *Global Biogeochemical Cycles*, **20** (3): 1-12, DOI: 10.1029/2005GB002559.

Eglinton, G., and Hamilton, R. J., 1967. Leaf epicuticular waxes. *Science*, **156** (3780): 1322-1335.

Ehleringer, J. R., Lin, Z. F., Filed, C. B., Sun, G. C., and Kuo, C. Y., 1987. Leaf carbon isotope ratios of plants from a subtropical monsoon forest. *Oecologia*, **72** (1): 109-114, DOI: 10.1007/s00442-015-3358-7.

Feng, J. L., Hu, M., Chan, C. K., Lau, P. S., Fang, M., He, L. Y., and Tang, X. Y., 2006. A comparative study of the organic matter in $PM_{2.5}$ from three Chinese megacities in three different climatic zones. *Atmospheric Environment*, **40** (21): 3983-3994, DOI: 10.1016/j.atmosenv.2006.02.017.

Feng, X., Benitez-Nelson, B. C., Monrlucon, D. B., Prahl, F. G., McNichol, A. P., Xu, L., Repeta, D. J., and Eglinton, T. I., 2013. ^{14}C and ^{13}C characteristics of higher plant biomarkers in Washington margin surface sediments. *Geochimica et Cosmochimica Acta*, **105**: 14-30, DOI: org/10.1016/j.gca.2012.11.034.

Feng, Z. D., Wang, L. X., Ji, Y. H., Guo, L. L., Lee, X. Q., and Dworkin, S. I., 2008. Climatic dependency of soil organic carbon isotope composition along the S-N Transect from 34°N to 52°N in central-east Asia. *Palaeogeography*, *Palaeoclimatology*, *Palaeoecology*, **257** (3): 335-343, DOI: 10.1016/j.palaeo.2007.10.026.

Games, L. M., Hayes, J. M., and Gunsalus, R. P., 1978. Methane producing bacteria: Natural fractionation of stable carbon isotopes. *Geochimica et Cosmochimica Acta*, **42** (8): 1295-1297, DOI: 10.1016/0016-7037(78)90123-0.

Gao, Y., Arimoto, R., Duce, R. A., Zhang, X. Y., Zhang, G. Y., An, Z. S., Chen, L. Q., Zhou, M. Y., and Gu, D. Y., 1997. Temporal and spatial distribution of dust and its deposition to the China Sea. *Tellus B*, **49** (2): 172-189, DOI: 10.1034/j.1600-0889.49.issue2.5.x.

Gelwicks, J. T., Risatti, J. B., and Hayes, J. M., 1994. Carbon isotope effects associated with acetoclastic methanogenesis. *Applied and Environmental Microbiology*, **60** (2): 467-472.

Guo, Z. G., Li, J. Y., Feng, J. L., Fang, M., and Yang, Z. S., 2006a. Compound-specific carbon isotope compositions of individual long-chain *n*-alkanes in severe Asian dust episodes in the North China coast in 2002. *Chinese Science Bulletin*, **51** (17): 2133-2140, DOI: 10.1007/s11434-006-2071-7.

Guo, Z. G., Sheng, L. F., Feng, J. L., and Fang, M., 2003. Seasonal variation of solvent extractable organic compounds in the aerosols in Qingdao, China. *Atmospheric Environment*, **37** (13): 1825-1834, DOI: 10.1016/S1352-2310(03)00064-5.

Guo, Z. G., Yang, Z. S., Lin, T., and Li, J. Y., 2006b. Compound-specific carbon isotope composition of individual *n*-alkane in the East China Sea mud areas. *Quaternary Sciences*, **26** (3): 384-390 (in Chinese).

Hedges, J. I., and Keil, R. G., 1995. Sedimentary organic matter preservation: An assessment and speculative synthesis. *Marine Chemistry*, **49** (2-3): 81-115, DOI: 10.1016/0304-4203(95)00008-F.

Hedges, J. I., and Oades, J. M., 1997. Comparative organic geochemistries of soil sand marine sediments. *Organic Geochemistry*, **27** (7-8): 319-361, DOI: 10.1016/S0146-6380(97)00056-9.

Kao, S. J., Lin, F. J., and Liu, K. K., 2003. Organic carbon and nitrogen contents and their isotopic compositions in surficial sediments from the East China Sea shelf and the southern Okinawa Trough. *Deep Sea Research Part II: Topical Studies in Oceanography*, **50** (6-7): 1203-1217, DOI: 10.1016/S0967-0645(03)00018-3.

Liu, K. B., 1988. Quaternary history of the temperate forests of China. *Quaternary Science Reviews*, **7** (1): 1-20, DOI: 10.1016/0277-3791(88)90089-3.

Liu, W. G., Ning, M., An, Z. S., Wu, Z. H., Lu, H. Y., and Cao, Y. N., 2002. Responses of organic carbon isotope to vegetation in the modern soil and paleo-soil of loess plateau. *Science in China (Series D)*, **32** (10): 830-836 (in Chinese with English abstract).

Lu, H. Y., Wu, N. Q., Gu, Z. Y., Guo, Z. T., Wang, L., Wu, H. B., Wang, G. A., and Zhou, L. P., 2004. Distribution of carbon isotope composition of modern soils in the Qinghai-Tibetan Plateau. *Biogeochemistry*, **70** (2): 273-297, DOI: 10.1023/B:BIOG.0000049343.48087.ac.

McKee, B. A., Aller, R. C., Allison, M. A., Bianchi, T. S., and Kineke, G. C., 2004. Transport and transformation of dissolved and particulate materials on continental margins influenced by major rivers: Benthic boundary layer and seabed processes. *Continental Shelf Research*, **24** (7-8): 899-926, DOI: 10.1016/j.csr.2004.02.009.

Milliman, J. D., Shen, H. T., Yang, Z. S., and Meade, R. H., 1985. Transport and deposition of river sediment in the Changjiang Estuary. *Continental Shelf Research*, **4** (1-2): 37-45, DOI: 10.1016/0278-4343(85)90020-2.

Pearson, A., McNichol, A. P., Benitez-Nelson, B. C., Hayes, J. M., and Eglinton, T. I., 2001. Origins of lipid biomarkers in Santa Monica Basin surface sediment: A case study using compound-specific $\Delta^{14}C$ analysis. *Geochimica et Cosmochimica Acta*, **65** (18): 3123-3137, DOI: 10.1016/S0016-7037(01)00657-3.

Qiao, S. Q., Yang, Z. S., Liu, J. P., Sun, X. X., Xiang, R., Shi, X. F., Fan, D. J., and Saito, Y., 2011. Records of late-holocene East Asian winter monsoon in the East China Sea: Key grain-size component of quartz versus bulk sediments. *Quaternary International*, **230** (1-2): 106-114, DOI: 10.1016/j.quaint.2010.01.020.

Rao, Z. G., Jia, G. D., Zhu, Z. Y., Wu, Y., and Zhang, J. W., 2008. Comparison of the carbon isotope composition of total organic carbon and long-chain *n*-alkane from surface soil in eastern China and their significance. *Chinese Science Bulletin*, **53** (24): 3921-3927, DOI: 10.1007/s11434-008-0296-3.

Uematsu, M., Wang, Z. F., and Uno, I., 2003. Atmospheric input of mineral dust to the western North Pacific region based on direct measurements and a regional chemical transport model. *Geophysical Research Letters*, **30** (6): 301-318, DOI: 10.1029/2002GL016645.

Wang, X. C., Sun, M. Y., and Li, A. C., 2008. Contrasting chemical and isotope compositions of organic matter in Changjiang (Yangtze River) estuarine and East China Sea shelf sediments. *Journal of Oceanography*, **64** (2): 311-321, DOI: 10.1007/s10872-008-0025-1.

Wang, Y. J., Lv, H. Y., Wang, G. A., Yang, H., and Li, Z., 2000. Carbon isotope analysis of C_3/C_4 plants and silicate of modern soil. *Chinese Science Bulletin*, **45** (9): 978-982 (in Chinese with English abstract).

Weijers, J., Schouten, S., Schefuß, E., Schneider, R. R., and Damsté, S., 2009. Disentangling marine, soil and plant organic carbon contributions to continental margin sediments: A multi-proxy approach in a 20,000 year sediment record from the Congo deep-sea fan. *Geochimica et Cosmochimica Acta*, **73** (1): 119-132, DOI: 10.1016/j.gca.2008.10.016.

Wu, Z. Y., 1980. *Vegetation of China*. Science Press, Beijing, 836-868 (in Chinese).

Wu, Y., Fu, Y., Zhang, Y., Pu, X., and Zhou, C., 2004. Phytoplankton distribution and its relation to the runoff in the Changjiang (Yangzte) Estuary. *Oceanologia et Limnologia Sinica*, **35** (3): 246-251 (in Chinese with English abstract).

Wu, Y., Zhang, J., Liu, S. M., Zhang, Z. F., Yao, Q. Z., Hong, G. H., and Cooper, L., 2007. Sources and distribution of carbon within the Yangtze River system. *Estuarine*, *Coastal and Shelf Science*, **71** (1-2): 13-25, DOI: 10.1016/j.ecss.2006.08.016.

Wu, Y., Eglinton, T., Yang, L. Y., Deng, B., Montluçon, D., and Zhang, J., 2013. Spatial variability in the abundance, composition, and age of organic matter in surficial sediments of the East China Sea. *Journal of Geophysical Research: Biogeosciences*, **118** (4): 1495-1507, DOI: 10.1002/2013JG002286.

Xing, L., Zhang, H. L., Yuan, Z. N., Sun, Y., and Zhao, M. X., 2011. Terrestrial and marine biomarker estimates of organic matter sources and distribution in surface sediments from the East China Sea shelf. *Continental Shelf Research*, **31** (10): 1106-1115, DOI: 10.1016/j.csr.2011.04.003.

Xing, L., Zhao, M. X., Gao, W. X., Wang, F., Zhang, H. L., Li, L., Liu, J., and Liu, Y. G., 2014. Multiple proxy estimates of source and spatial variation in organic matter in surface sediments from the southern Yellow Sea. *Organic Geochemistry*, **76**: 72-81, DOI: 10.1016/j.orggeochem.2014.07.005.

Yamamoto, S., Kawamura, K., Seki, O., Kariya, T., and Lee, M., 2013. Influence of aerosol source regions and transport pathway on δD of terrestrial biomarkes in atmospheric aerosols from the East China Sea. *Geochimica et Cosmochimica Acta*, **106**: 164-176, DOI: 10.1016/j.gca.2012.12.030.

Yang, B., Cao, L., Liu, S. M., and Zhang, G. S., 2015. Biogeochemistry of bulk organic matter and biogenic elements in surface sediments of the Yangtze River Estuary and adjacent sea. *Marine Pollution Bulletin*, **96** (1-2): 471-484, DOI: 10.1016/j.marpolbul.2015.05.003.

Yang, L. Y., Wu, Y., Zhang, J., Yu, H., Zhang, G. S., and Zhu, Z. Y., 2008. Distribution of lignin and sources of organic matter in surface sediments from the adjacent area of the Changjiang Estuary in China. *Acta Oceanologica Sinica*, **30** (5): 35-42 (in Chinese with English abstract).

Yao, P., Yu, Z. G., Bianchi, T. S., Guo, Z. G., Zhao, M. X., Knappy, C. S., Keely, B. J., Zhao, B., Zhang, T. T., Pan, H. H., Wang, J. P., and Li, D., 2015. A multiproxy analysis of sedimentary organic carbon in the Changjiang Estuary and adjacent shelf. *Journal of Geophysical Research: Biogeosciences*, **120** (7): 1407-1429, DOI: 10.1002/2014JG002831.

Yi, S. H., Saito, Y., and Yang, D. Y., 2006. Palynological evidence for Holocene environmental change in the Changjiang (Yangtze River) Delta, China. *Palaeogeography*, *Palaeoclimatology*, *Palaeoecology*, **241** (1): 103-117, DOI: 10.1016/j.palaeo.2006.06.016.

Zhang, C. J., Chen, F. H., and Jin, M., 2003a. Study on modern plant C-13 in Western China and its significance. *Chinese Journal Geochemistry*, **22** (2): 97-106, DOI: 10.1007/BF02831518.

Zhang, G. S., Zhang, J., and Liu, S. M., 2007. Characterization of nutrients in the atmospheric wet and dry deposition observed at the two monitoring sites over Yellow Sea and East China Sea. *Journal of Atmospheric Chemistry*, **57** (1): 41-57, DOI: 10.1007/s10874-007-9060-3.

Zhang, Z. H., Zhao, M. X., Lu, H. Y., and Faiia, A. M., 2003b. Lower temperature as the main cause of C_4 plant declines during the glacial periods on the Chinese Loess Plateau. *Earth and Planetary Science Letters*, **214** (3-4): 467-481, DOI: 10.1016/S0012-821X(03)00387-X.

Zhao, M. X., Eglinton, G., Haslett, S. K., Jordan, R. W., Sarnthein, M., and Zhang, Z. H., 2000. Marine and terrestrial biomarker records for the last 35,000 years at ODP 658C off NW Africa. *Organic Geochemistry*, **31** (9): 919-930, DOI: 10.1016/S0146-6380(00)00027-9.

Zhu, C., Wagner, T., Talbot, H. M., Weijers, J., Pan, J. M., and Pancost, R. D., 2013. Mechanistic controls on diverse fates of terrestrial organic components in the East China Sea. *Geochimica et Cosmochimica Acta*, **117**: 129-143, DOI: 10.1016/j.gca.2013.04.015.

Zhu, C., Xue, B., Pan, J. M., Zhang, H. S., Wagner, T., and Pancost, R. D., 2008. The dispersal of sedimentary terrestrial organic matter in the East China Sea as revealed by biomarkers and hydro-chemical characteristics. *Organic Geochemistry*, **39** (8): 952-957, DOI: 10.1016/j.orggeochem.2008.04.024.

(Edited by Ji Dechun)